

Polyaniline/TiO₂ Nanocomposite: Enzymatic Synthesis and Electrochemical Properties

Mohammad Reza Nabid^{1,*}, Maryam Golbabaee¹, Abdolmajid Bayandori Moghaddam², Rassoul Dinarvand², Roya Sedghi¹

¹Department of Chemistry, Faculty of Science, Shahid Beheshti University G. C., 1983963113, Tehran, Iran

²Medical Nanotechnology Research Centre, Faculty of Pharmacy, Tehran University of Medical Sciences, Tehran, P.O. Box 14155-6451, Iran

*E-mail: m-nabid@sbu.ac.ir

Received: 23 July 2008 / Accepted: 8 August 2008 / Published: 8 September 2008

An enzymatic route for synthesis of a conducting nanocomposite between Polyaniline (PANI) and anatase TiO₂ nanoparticles (NPs) is presented. The presence of sulfonated polystyrene (SPS) affects the polymerization reaction. Horseradish peroxidase (HRP) was used to catalyze the polymerization. Polyaniline was deposited on the surface of TiO₂ NPs, forming a core-shell structure. Enzymatically synthesized nanocomposite was characterized by FT-IR spectroscopy, UV-Vis. spectroscopy and scanning electron microscopy (SEM). The results indicate that a strong interaction exist at the interface of PANI and nano-TiO₂. The ability of PANI and PANI/TiO₂ NPs for electron exchange by Platinum (Pt) electrode, by casting the PANI and PANI/TiO₂ NPs on the Pt electrode surface was assessed by cyclic voltammetry. Difference of anodic and cathodic peak potential and formal potential values for PANI (281 mV and 425.5 mV, respectively) and PANI/TiO₂ NPs (39 mV and 591.5 mV, respectively) were deduced by the analysis of voltammograms.

Keywords: Enzymatic polymerization; Nanocomposite; Conducting polymers; Horseradish peroxidase, TiO₂ nanoparticles

1. INTRODUCTION

Conducting polymers have drawn considerable interest for their wide applications. PANI is one of the most attractive conducting polymers due to the high conductivity and good stability [1]. Inorganic nanoparticles such as TiO₂ have so far been encapsulated into the shell of conducting polymers giving rise to a host of nanocomposite [2]. Also PANI/TiO₂ nanocomposite has attracted more attention in recent years [3]. Xia and Wang [4] prepared PANI/TiO₂ nanocomposite by ultrasonic

irradiation. Schnitzler and Zarbin [5] obtained hybrid materials of TiO₂ nanoparticles and PANI based on sol-gel technique. The introduction of PANI not only improves the conductivity of TiO₂ nanoparticles but also improve the dispersibility of TiO₂ nanoparticles in macromolecules.

Polymers with well-defined structures can be prepared by enzyme-catalyzed in an environmentally benign process [6]. An enzymatic polymerization approach was developed in which HRP was used as a catalyst and H₂O₂ as an oxidating agent [7, 8]. The enzymatic polymerization of aniline is followed in the presence of a polyelectrolyte such as SPS [9]. Mechanism of enzymatic polymerization of aniline in the presence of SPS is shown in Figure 1. Template-assisted enzymatic polymerization of aniline represents a great advantage in PANI processability and stable solutions of doped PANI can be obtained in this method [10].

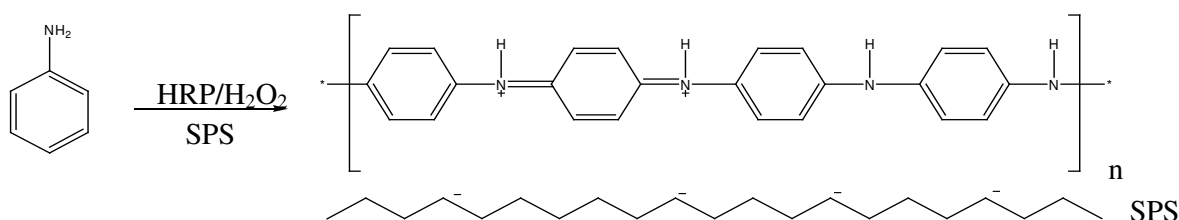


Figure 1. Enzymatic polymerization mechanism of aniline in the presence of SPS.

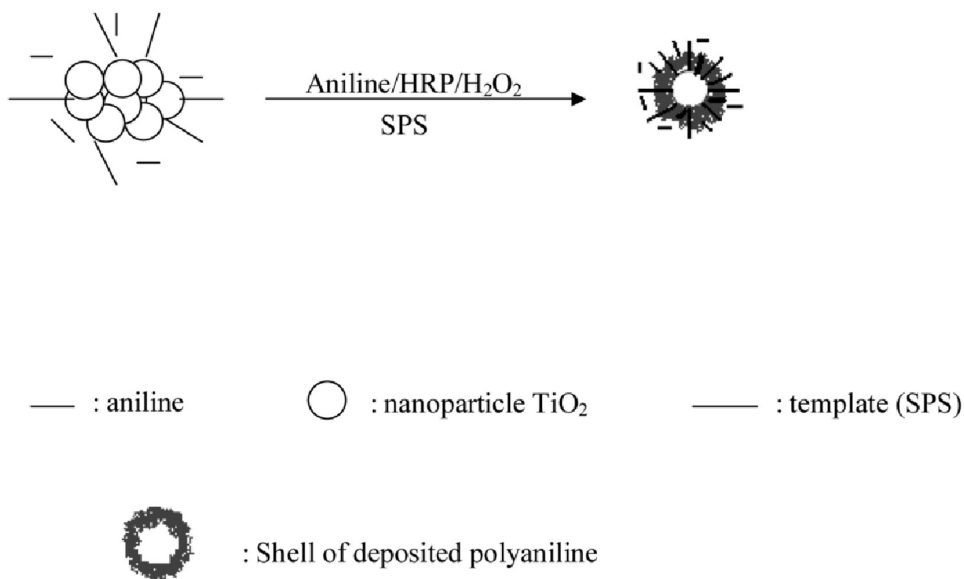


Figure 2. PANI/TiO₂ nanocomposite formation.

In this work, our aim was formation of electrostatic complex between aniline monomers and polyelectrolyte on anatase TiO₂ NPs surface. Then, after addition of enzyme, the polymerization of aniline took place. Encapsulation of inorganic nanoparticles inside the shell of conducting polymers is the most attractive aspect in this synthesis. The template is used in order to control the shape of nanoparticles. The nanocomposite formation in the presence of template or surfactant is visualized in Figure 2.

2. EXPERIMENTAL PART

2.1. Materials

Horseradish peroxidase (EC 1.11.1.7) (about 170 units/mg), hydrogen peroxide (30 wt %), aniline, titanium (IV) chloride and other reagents obtained from Merck. Sulfonated polystyrene was obtained from Aldrich. However, anatase TiO₂ NPs was prepared in our laboratory.

2.2. Preparation of TiO₂ nanoparticles

For the preparation of TiO₂ NPs, a solution of 1.5 M ammonium sulfate which consisted of 0.75 M titanium (IV) chloride was used. The total volume of 50 mL in aqueous solution was heated at 75 °C and maintained at the same temperature for 90 min. After that, ammonium hydroxide solution (2.5 M) was added drop-wise under high speed stirring until the pH reached to 7.0. The precipitated titanium hydroxide was collected, repeatedly washed with distilled water and ethanol and dried at 50-55 °C. After being calcined at 400 °C for 4 h, the sample was slowly cooled at room temperature.

2.3. Preparation of PANI/ TiO₂ nanocomposite

5 μL (0.06 mmol) aniline was injected to 7.5 ml phosphate buffer pH 4.3 containing 50 mg nano-TiO₂ with constant stirring for 15 min at room temperature. To reduce aggregation of anatase-TiO₂ nanoparticles, ultrasonic action was needed for 30 min. Then 0.0009 g (0.004 mmol) SPS (based on molecular repeat unit) was added to the solution and stirred for 30 min, afterward 0.5 mg HRP was added to the solution. To start polymerization, diluted H₂O₂ was used. During 60 min, 2.25 ml (0.02 M) H₂O₂ was added drop-wise with constant stirring. After 24 h, the reaction mixture was filtered with sinter-glass and dried in vacuum oven at 60 °C for 24 h and a fine tint green powder was obtained.

2.4. Analytical techniques

The scanning electron microscopic images were recorded using Cambridge scanning electron microscope model stereo scan 360 and the transmission electron microscopic studies were performed using a Phillips transmission electron microscope. FT-IR measurements were carried out on a

BRUKER IFS 66/S FT-IR spectrometer in the form of dried samples by using KBr pellets. Solid-state UV-Vis spectra were recorded on a Shimadzu 2100 spectrophotometer in the range of 200-900 nm, and BaSO₄ was used as a reference. The cyclic voltammetric (CV) measurements were performed using a Metrohm computerized voltammetric model 747. CVs were recorded at room temperature by employing a three-electrode cell with platinum as an auxiliary electrode, an Ag/AgCl electrode as the reference electrode and platinum disk (d=1.8 mm) as the working electrode. The CVs were obtained in 1.0 M HCl electrolyte by casting the nanocomposite on platinum working electrode and scanned between 0 to 1.0 V at scan rates between 50 to 200 mV/s. Thermogravimetric analysis (TGA) was carried out using STA 1500 instrument at a heating rate of 10 °C min⁻¹ in air.

3. RESULTS AND DISCUSSION

3.1. Fourier- transform infrared spectra

FT-IR spectra of TiO₂ and PANI/TiO₂ were shown in Figure 3(a) and (b). In addition to observed peaks due to TiO₂ in Figure 3(a), the main characteristic bands of polyaniline were seen in Figure 3(b). The band at 3450 cm⁻¹ is attributable to N-H stretching. The bands at 1577 and 1485 cm⁻¹ corresponded to quinoid and benzenoid structure of PANI, respectively. Also the band at 1310 cm⁻¹ assigned to C-N stretching of a secondary aromatic amine. The peaks at 1035 and 1009 cm⁻¹ belong to asymmetric and symmetric S=O stretching and this confirms the presence of SPS in the complex. Because titanium is a transition metal, it has intense tendency to form coordination compound with nitrogen atom in PANI macromolecule. This interaction may weaken the bond strengths of C=N, C=C and C-N in PANI macromolecule. These results confirm to the presence of PANI and SPS in nanocomposite.

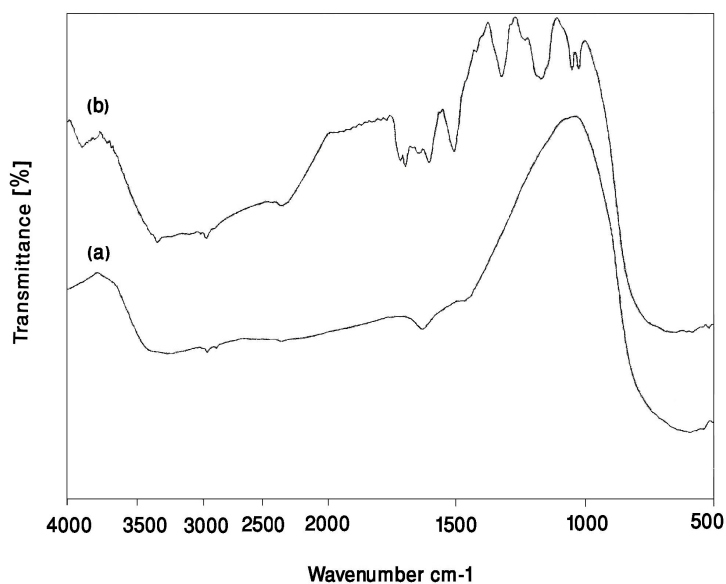


Figure 3. FT-IR spectra of a) TiO₂ and b) PANI/TiO₂ nanocomposite.

3.2. UV-Vis. spectroscopy

The UV-Vis spectrum of the PANI doped with SPS and reflectance spectrum of PANI/TiO₂ nanocomposite is shown in Figure 4(a) and (b). In Figure 4(a) the three characteristic bands of doped PANI with SPS appear at about 365, 480 and over 820 nm, which are attributed to the π - π^* , polaron- π^* and π -polaron transitions, respectively. From Figure 4(b), it can be seen that the prepared nanocomposite can strongly absorb the UV and visible light. The hybrid samples present characteristic bands of PANI at about 380, 460 and over 820 nm. Moreover, the peak at over 480 nm in PANI doped with SPS is obviously shifted to 460 nm in nanocomposite. It indicates that encapsulation of TiO₂ NPs has the effect on doping of conducting polyaniline. This shift shows shortening in the conjugation length that reported previously [11] or may be the coordinating complex formation between TiO₂ NPs and PANI chains.

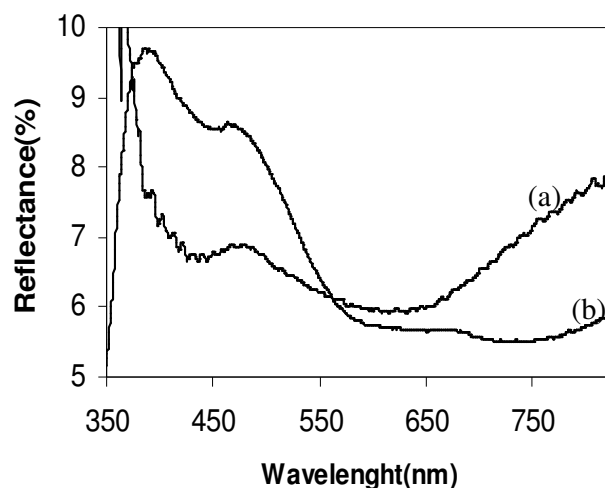


Figure 4. UV-Vis spectra of (a) PANI doped with SPS and (b) PANI/TiO₂ NPs composite complex.

3.3. Cyclic voltammetry

A number of investigations carried out to find applications of nanomaterials in electrochemical studies could impart strong electrocatalytic activity to some important biomolecules [12-14].

The integrity of the PANI and PANI/TiO₂ NPs construction were assessed by cyclic voltammetry (CV). A macroscopic electrode was required to attain a large enough sample to yield detectable direct oxidation and reduction currents. The comparative CVs for the PANI and PANI/TiO₂ NPs in 1.0 M HCl were obtained. These voltammograms are demonstrated in Figure 5. Figure 5(a) depicts a well-defined pair of oxidation-reduction (redox) peaks observed at the PANI/Pt electrode at 50 mV/s. The PANI/Pt electrode presented the oxidative peak potential at 566 mV, which related to reductive peak potential at 285 mV, indicating the presence of PANI at the Pt electrode surfaces. The difference between anodic and cathodic peak potential values was $\Delta E = 281$ mV. The formal potential

for the PANI/Pt electrode was 425.5 mV with respect to the reference electrode. Additionally, oxidative and reductive peak potentials, ΔE and formal potential values for the PANI/TiO₂ NPs/Pt electrode are 611, 572, 39 and 591.5 mV, respectively. It was concluded that the TiO₂ NPs could play a key role in the observation of PANI voltammetric response. These nanoparticles displayed a great effect on the electron exchange assistance, because the reversibility is better for PANI/TiO₂ NPs/Pt electrode with the ΔE value of 39 mV in comparison to that of PANI/Pt electrode with the ΔE value of 281 mV. To further investigate, the effect of scan rates on the voltammetric behavior of PANI/Pt and PANI/TiO₂ NPs/Pt electrodes were studied in details. Figures 5(b) and (c) depicts the CVs for above mentioned electrodes at various scan rates.

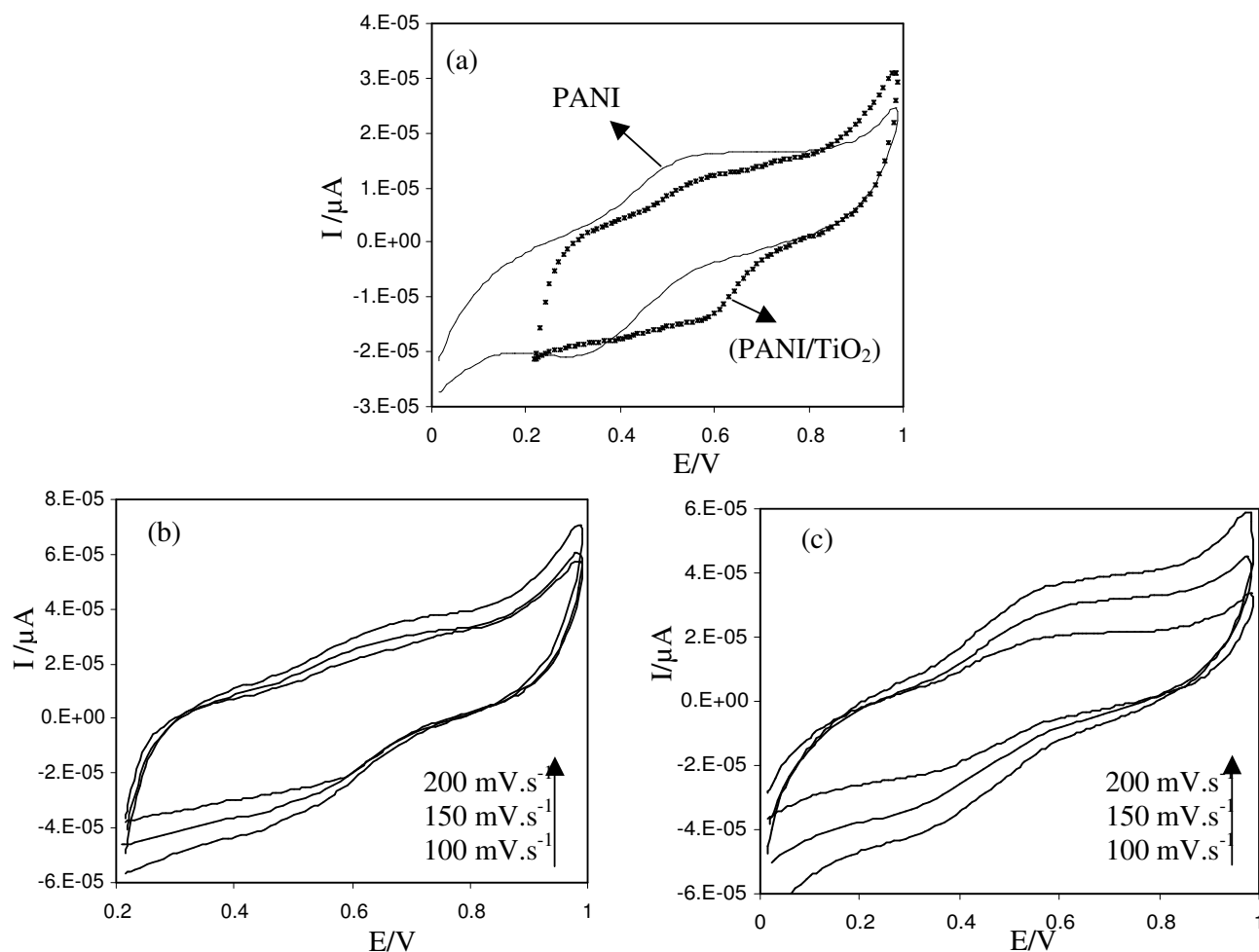


Figure 5. (a) Comparative cyclic voltammograms of PANI/Pt and PANI/TiO₂ NPs/Pt electrodes at 50 mV/s, (b) PANI and (c) PANI/TiO₂ NPs/Pt electrode at different scan rates.

3.4. Morphological characterization

Morphological studies were done with SEM and TEM, which confirm the formation of nanocomposite. Scanning electron micrographs of TiO₂ nanoparticles are shown in Figure 6(a) and PANI/TiO₂ nanocomposite in Figure 6(b). Comparing these images showed that the growing of PANI

on TiO_2 NPs surfaces. Figure 7 shows the TEM image of PANI/ TiO_2 NPs. In accordance to our studies, after enzymatic polymerization of aniline in the presence of TiO_2 NPs, dimension increased almost 5-7 nm. As shown in SEM and TEM images, polyaniline layers on the TiO_2 NPs surface attached together and generated the porous PANI/ TiO_2 nanocomposite. In fact, such structure has been created from the TiO_2 NPs presence in the course of enzymatic polymerization process. This is a result of polymer growth on the surface of nanoparticles. In addition, it is easy to control the composite structure using various types and shapes of metal oxide nanomaterials. Since composites made from metal oxide nanomaterials exhibit essential stability (owing to metal oxide nanomaterial structures) and polymer film growth is efficiently stable, this approach can be successfully employed for applied purposes.

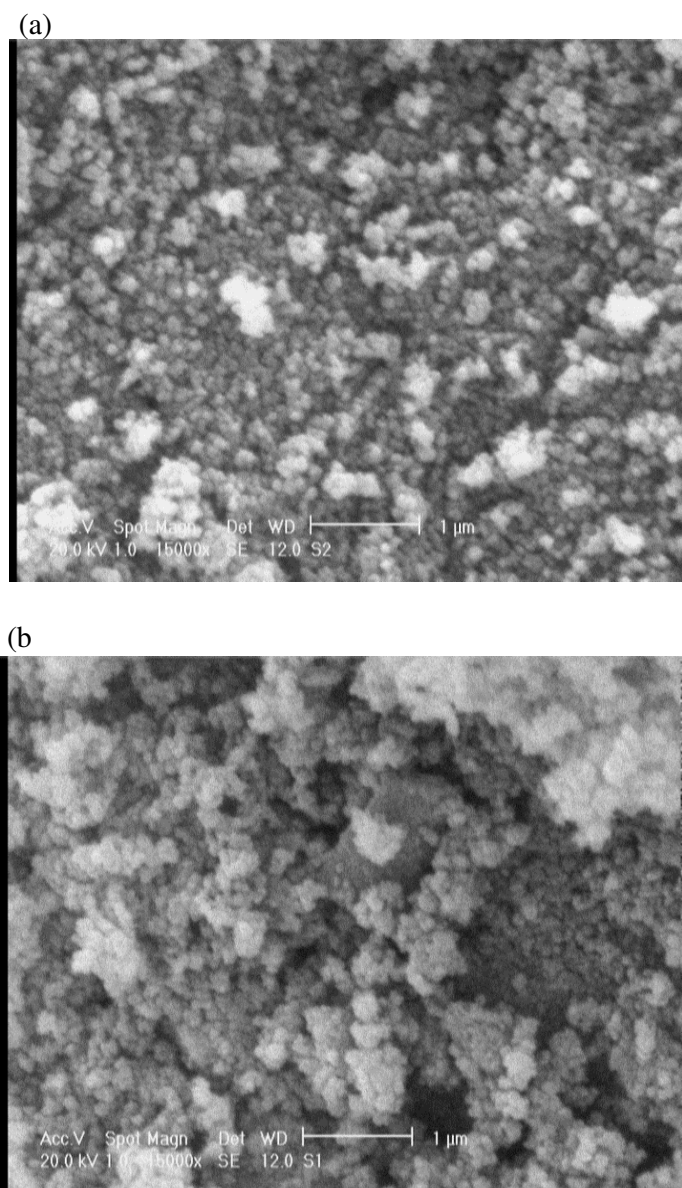


Figure 6. SEM images of (a) anatase TiO_2 NPs and (b) PANI/ TiO_2 NPs composite.

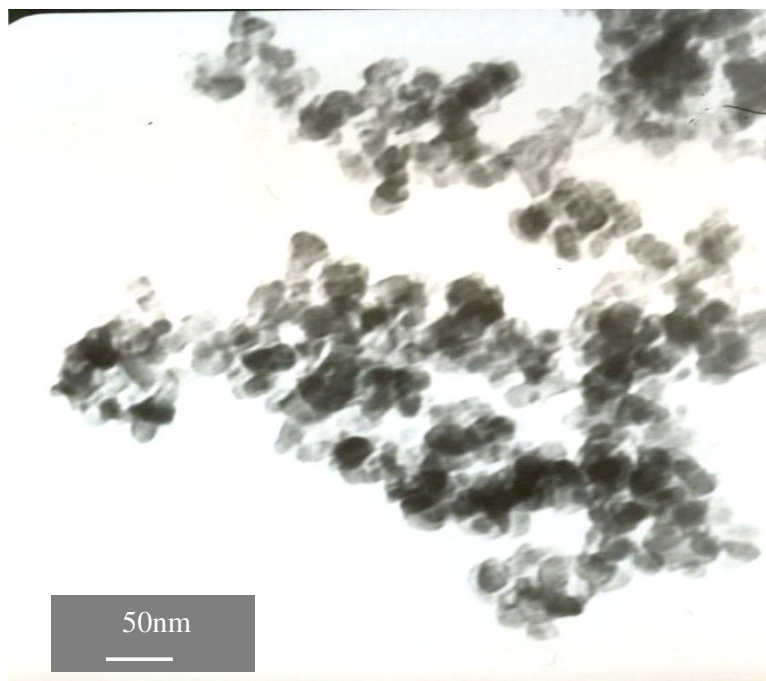


Figure 7. TEM image of PANI/TiO₂ NPs composite.

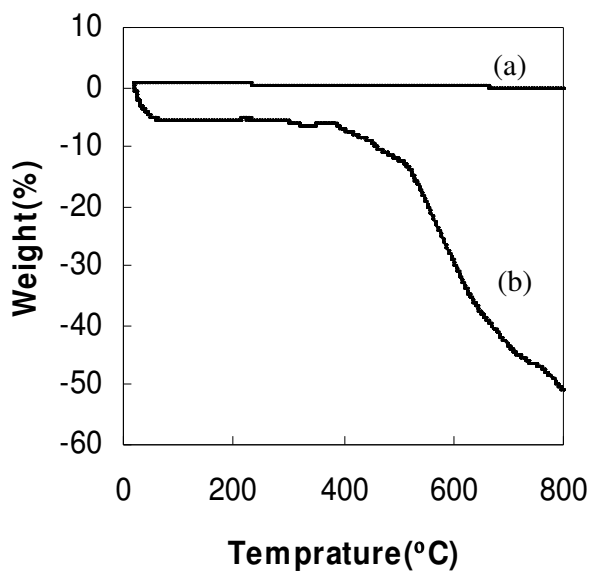


Figure 8. Thermogravimetric curves of TiO₂ NPs (curve (a)) and PANI/TiO₂ NPs composite (curve (b)).

3.5. Thermogravimetric analysis (TGA)

The thermal behavior of the TiO₂ NPs and PANI/TiO₂ NPs composite samples were investigated by TGA, and the results are shown in Figure 8. In this Figure, curve (a) shows that TiO₂

NPs is very stable in air and no decomposition takes place in the range of 20-800 °C. The thermogravimetric curve of PANI/TiO₂ is shown in Figure 8(b). The results show that the trend of PANI/TiO₂ NPs composite degradation is similar to PANI [15] but the thermal stability of enzymatically synthesized nanocomposite is lower than chemically synthesized PANI probably due to some chain defect [16, 17]. These chain defects are produced because of the higher pH conditions employed during the enzymatic synthesis. The first weight loss observed at 80 °C was essentially due to desorption of water absorbed on the doped polymer. This curve also indicates that there is a sharp weight loss near 430 °C and continues until 660 °C, which is attributed to degradation of skeletal polyaniline chain structure [18]. The temperature of thermal decomposition of polyaniline in PANI/TiO₂ NPs composite is about 430 °C which is lower than pure polyaniline at 480 °C. These results indicate that a strong interaction exist at the interface of PANI and TiO₂ NPs which probably weakens the interaction of inter-chains in PANI, that leads to thermal degradation of polyaniline. TG analysis indicates that the nanocomposite contains 25% conducting PANI by mass.

4. CONCLUSIONS

A PANI/TiO₂ nanocomposite was successfully obtained by in-situ enzymatic polymerization of aniline in the presence of SPS and TiO₂ NPs as a template and nanoparticle, respectively. Polymerization was carried out by horseradish peroxidase (HRP) in the presence of hydrogen peroxide. Polyaniline was deposited on the surface of TiO₂ NPs forming a core-shell structure. The nanocomposite results were determined with SEM, FT-IR, CV and TGA which confirmed the formation of PANI/TiO₂ nanocomposite.

References

1. S. Palaniappan, *Eur. Polym. J.* 37(2001) 975.
2. L. J. Zang, M. X. Wang, *J. Phys. Chem.* 107(2003) 6748.
3. R. Gangopadhyay, A. De, *Chem. Mater.* 12 (2000) 608.
4. H. Xia, Q. Wang, *Chem. Mater.* 14 (2002) 2158.
5. D. C. Schnitzler, M. S. Meruvia, I. A. Hummlgen, A. J. Z. G. Zarbin, *J. Brazil. Chem. Soc.* 15 (2004) 378.
6. R. A. Gross, R. Kumar, B. Kalra, *Chem. Rev.* 101 (2001) 2097.
7. V. Rumbau, J. A. Pomposo, J. A. Alduncin, H. Grande, D. Mecerreyes, E. Ochoteco, *Enzyme Microb. Technol.* 40(2007)1412.
8. M. R. Nabid, R. Sedghi, A. A. Entezami, *J. Appl. Polym. Sci.* 103(2007) 3724.
9. W. Liu, J. Kumar, S. Tripathy, K. J. Senecal, L. Samuelson, *J. Am. Chem. Soc.* 121 (1999) 71.
10. R. Cruz-silva, J. Romero-Garcia, J. L. Angulo-Sanchez, E. Flores-Loyola, M. H. Farias, F. F. Castillon, J. A. Diaz, *Polymer* 45 (2004) 4711.
11. R. Cruz-silva, J. Romero-Garcia, J. L. Angulo-Sanchez, E. Flores-Loyola, M. H. Farias, F. F. Castillon, J. A. Diaz, *Polymer* 45 (2004) 4711.

12. A. Bayandori Moghaddam, M. Kazemzad, M. R. Nabid, H. H. Dabaghi, *Int. J. Electrochem. Sci.* 3 (2008) 291.
13. P. Xiao, W. Wu, J. Yu, F. Zhao, *Int. J. Electrochem. Sci.* 2 (2007) 149.
14. A. Bayandori Moghaddam, M. R. Ganjali, R. Dinarvand, S. Ahadi, A. A. Saboury, *Biophys. Chem.* 134 (2008) 25.
15. X. W. Li, W. Chen, C. Q. Bian, J. B. He, N. Xu, G. Xue, *Appl. Surf. Sci.* 217 (2003) 16.
16. A. J. Milton, A. P. Monkman, *J. Phys. D: Appl. Phys.* 26 (1993) 1468.
17. R. Cruz-silva, C. Ruiz-Flores, L. Arizmendi, J. Romero-Garcia, E. Arias-Marin, I. Moggio, F. F. Castillon, M. H. Farias, *Polymer* 45 (2004) 4711.
18. C. S. Danielle, S. M. Michelle, A. H. Ivo, J. G. Z. Aldo, *Chem. Mater.* 15 (2003) 4658.